2013 European Control Conference (ECC)
July 17-19, 2013, Zürich, Switzerland.

Controller Design and Evaluation for Vehicle Run-Off-the-Road and Recovery

Matthew Jensen, Ph.D., Paul Freeman, John Wagner, Ph.D., P.E., and Kim Alexander, Ed.D.

Abstract— **Run-off-the-road (ROR) and unsuccessful recovery events account for a significant percentage of fatal vehicle crashes. Changes to roadway infrastructure have reduced the severity of automotive crashes; however, it is driver performance which remains a primary contributing factor to these incidents. An on-board vehicle control system, using combined steering and differential braking, provides enhanced safety by removing driver error from the recovery process once the ROR event has been identified. In this study, two control algorithms, based on sliding mode and state flow theories, have been designed to automatically recover a vehicle from this dangerous scenario. A driver model was also developed based on experimental data gathered at a tire manufacturer's test track. The controllers were numerically evaluated for a common road departure and return situation with comparison to the empirical driver model. The results show that both controllers safely recovered the vehicle and outperformed the driver steering model. Specifically, the state flow controller reduced recovery time by 40% compared to the sliding mode controller, while the driver model resulted in vehicle spin out.**

I. Introduction

As the number of vehicles on roadways around the world rises each year, transportation safety becomes an ever increasing concern. One of the leading types of fatal crashes involves the vehicle traveling off the roadway, and is typically referred to as run-off-the-road (ROR). In 2008, the U.S. Department of Transportation reported that 65% of all fatal single-vehicle crashes occured off the roadway or on the shoulder [1].

Statistically, the most significant factors leading to ROR crashes include driver inattention, fatigue, intoxication, and road conditions [2]. Present solutions to these factors involve roadway infrastructure modifications [3], including the use of rumble strips placed just outside the edge of the lane [4], wider shoulders to provide the driver with more room before leaving the paved surface, and guardrails and tension cables to keep the vehicle from colliding with more harmful objects [5]. While these methods have been proven to help reduce the occurrence of ROR crashes [4], not all roads can be retrofitted with these modifications and the issue of driver performance is not directly addressed.

To supplement roadway modifications, vehicle safety systems have also been investigated to assist the driver in avoiding ROR occurrences. One example is the lane-departure warning system (LDWS). In [6], an LDWS is designed using the vehicle's operational states to detect driver inattention. The results show that 70% of redundant lane departure warnings were suppressed using this technique. A lane-keeping controller, to aid drivers in maintaining lane-centered positioning, was developed in [7], for a steer-by-wire equipped vehicle. The stability and performance guarantees of the lane-keeping controller were demonstrated using a Lyapunov function [8]. In [9], a two-degree-of-freedom vehicle chassis model was used to analyze the vehicle dynamics during an ROR event; a steering controller aided the driver during recovery. Successful results were demonstrated as the vehicle yaw angle was decreased by 30%, and the reaction window in which the driver could perform the recovery was increased by 75%.

One of the primary drawbacks of these driver assist systems is that they depend on correct or near correct driver behaviors. Research studies show that improper driver inputs are the leading cause of many ROR crashes [2]. With the advancement of vehicle technology, there exists an opportunity to create a controller that is capable of performing an autonomous ROR recovery using combined steering and braking. This paper investigates autonomous control of vehicle steering and braking as a means of directly isolating the primary source of error in ROR crashes and increasing occupant safety.

II. Vehicle Models

The on-board controllers described in the subsequent sections rely on the provision of the vehicle's operational states and dynamics. This requirement necessitates the establishment of a mathematical model which adequately represents the vehicle behavior. For this study, a seven degree-of-freedom vehicle model has been selected [10]. The equations of motion for the vehicle chassis are given as

$$\begin{aligned} m\ddot{x} = {} & (F_{xfl} + F_{xfr})\cos(\delta) + F_{xrl} + F_{xrr} \\ & - (F_{yfl} + F_{yfr})\sin(\delta) + m\dot{\psi}\dot{y} \end{aligned} \tag{1}$$

$$\begin{aligned} m\ddot{y} = {} & F_{yrl} + F_{yrr} + (F_{xfl} + F_{xfr})\sin(\delta) \\ & + (F_{yfl} + F_{yfr})\cos(\delta) - m\dot{\psi}\dot{x} \end{aligned} \tag{2}$$

$$\begin{aligned} I_z\ddot{\psi} = {} & \ell_f[(F_{xfl} + F_{xfr})\sin(\delta) + (F_{yfl} + F_{yfr})\cos(\delta)] \\ & - \ell_r(F_{yrl} + F_{yrr}) + 0.5\ell_w[(F_{xfr} - F_{xfl})\cos(\delta) \\ & + (F_{xrr} - F_{xrl}) + (F_{yfl} - F_{yfr})\sin(\delta)] \end{aligned} \tag{3}$$

M. Jensen is with the School of Engineering, University of North Florida, Jacksonville, FL 32224 USA (email: mjensen@clemson.edu)

P. Freeman is with the Department of Mechanical Engineering, Clemson University, Clemson, SC 29634 USA (email: ptfreem@clemson.edu)

J. Wagner is with the Department of Mechanical Engineering, Clemson University, Clemson, SC 29634 USA (corresponding author, phone: 864-656-7376; fax: 864-656-4435; email: jwagner@clemson.edu)

K. Alexander is with the Automotive Safety Research Institute, Clemson University, Clemson, SC 29634 USA (email: kalxndr@clemson.edu)

where m, I_z, and δ are the vehicle's mass, moment of inertia, and wheel steering angle, respectively. The yaw, ψ, is the angle of the vehicle's center line relative to an Earth-fixed reference frame, and ℓ_f and ℓ_r are the distances from the vehicle's center of gravity (CG) to the front and rear axles. The lateral distance between the left and right wheels is given by ℓ_w and the tire force, F, includes subscripts denoting in order, body-axis direction (x, y), longitudinal position (front, rear), and lateral position (left, right).

The controller development procedure assumes that the vehicle is equipped with both steer-by-wire and brake-by-wire systems. Implementation of the steering system was assumed to be similar to that presented in [11]. To control the system feedback and rack motor actuators, a classical feedback controller along with feed-forward, friction, and aligning moment compensation was selected. Using this controller, the required steering actuator torque, τ, can be related to the desired steering wheel angle, θ_d, as

$$\begin{aligned}\tau = K_p(\theta_d - \theta) + K_d(\dot{\theta}_d - \dot{\theta}) + J_s\ddot{\theta}_d \\ + b_s\dot{\theta}_d + F_s sgn(\dot{\theta}_d) + k_a\hat{\tau}_a\end{aligned} \tag{4}$$

where K_p, K_d, and k_a are controller gains, θ is the actual steering wheel angle, $\hat{\tau}_a$ is the aligning moment, and J_s, b_s, and F_s denote the system inertia, damping, and Coulomb friction constants.

Numerous research has been conducted on electronic brake-by-wire systems [12], [13]. One of the direct methods includes the use of an eddy current machine to execute the braking requirements. A study performed in [14] showed that for variations in angular wheel speed of less than 500RPM (60km/h assuming a rolling radius of $r_{eff} = 0.359m$), the torque generated by the machine, τ_{brake}, is fairly linear with respect to lower current levels ($i_{brake} < 150A$). It was assumed that the top vehicle speed varied between $50 < V_{CG} < 100km/h$ and $i_{brake} \leq 150A$, hence, the braking torque applied to the vehicle was $\tau_{brake} = k_b \cdot i_{brake}$ where k_b is a known constant.

III. Controller Development

The safe recovery of a vehicle from an ROR event requires different steering and braking strategies depending on the stage of the recovery process. Fig. 1 illustrates the critical moments in an ROR situation based upon vehicle behavior and the ideal actions undertaken by the controllers. The vehicle transitions from normal driving to a two or four-wheels-off situation between time t_1 and t_2. At t_2, the controller attempts to decelerate and stabilize the vehicle through moderate differential braking. Next, assuming vehicle travel on the right side of the road and departure likewise, a counter-clockwise (CCW) steering input and reduced braking is implemented from time t_3 to t_4. As the wheels return to the roadway, the steering input is reduced until all four wheels have returned at t_5. Finally, a clock-wise (CW) steering input orients the vehicle within the driving lane as shown at time t_6.

The coupled nonlinear dynamics described by the vehicle chassis, steering, and braking models justify the need for nonlinear control strategies. Sliding mode (SM) control is an appealing candidate for its robust properties and method of replacing complex higher-order dynamics with equivalent 1st-order problems [15]. It is well suited to handle and manipulate the coupled dynamics of the nonlinear vehicle system to produce desired results. The multi-phased nature of the ROR recovery process makes state flow (SF) an ideal choice for an autonomous controller. In both cases, independent and cooperative steering and braking are necessary to safely return the vehicle to the roadway without driver involvement.

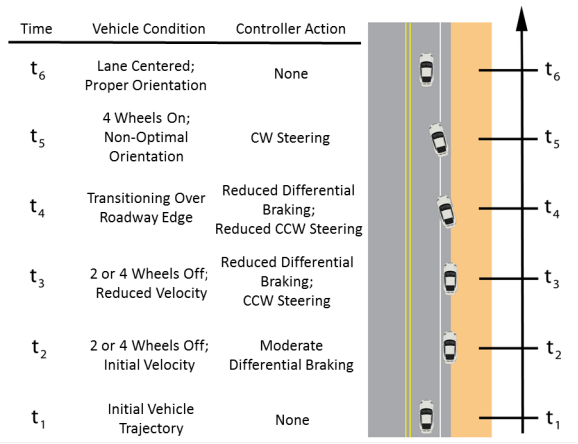

Fig. 1: Ideal controller actions during crucial phases of a run-off-the-road (ROR) and recovery event

A. Sliding Mode Controller

The goal of the steering controller is to guide the vehicle back onto the roadway, aligning it in the center of the lane, parallel to the road. The proposed SM steering controller is based on a potential field lane-keeping (L-K) controller developed in [7]. The controller determines the proper steer angle needed to maintain the vehicle within the prescribed lane through use of sensory data and GPS. It is assumed that the vehicle is equipped with the necessary sensors and the steering inputs are implemented through a steer-by-wire system. The desired steering angle is based on the quadratic error function, V, given as

$$V = k(e + x_{la}\sin\psi)^2 \tag{5}$$

where k is the potential field gain, $e = y_{CG} - y_{LC}$ is the lateral vehicle position error, and $x_{la}\sin\psi$ is the vehicle heading error. The variable y_{LC} is the lane center's lateral position, and x_{la} denotes the projection distance.

The front wheel steering angle, δ, is determined by

$$\delta = \frac{1}{C_f}\frac{\partial V}{\partial e}\cos\psi \tag{6}$$

where C_f is the front cornering stiffness [8]. As previously stated, the recovery steering commands are based solely on the L-K controller and not on the driver's inputs.

To supplement the commanded steering inputs of the L-K controller, a differential braking strategy was utilized to introduce a yaw moment, $M_{\psi b}$, through a brake-by-wire

system. To avoid conflicting with the steering controller, the commanded steering angle was used as an input to the braking controller. This way, braking performed by the controller would assist, rather than oppose, the steering action. For example, when a CW steer angle is commanded, the braking controller will apply the right-side brake to produce a CW yaw moment.

The SM brake controller relies on the definition of a sliding surface or a geometrical locus upon which the controller applies high frequency switching to create a controller boundary. A number of SM differential braking controllers have been developed, each with a unique sliding surface, s [10], [16], [17]. The most prevalent surfaces consider a weighted combination of the vehicle sideslip angle, β, sideslip angular velocity, $\dot{\beta}$, and yaw rate, $\dot{\psi}$. For this study, the chosen sliding surface is described as

$$s = \dot{\psi} - \dot{\psi}_{target} + \xi(\beta - \beta_{target}) \tag{7}$$

where the parameter ξ denotes a weighting factor. Note that the sliding surface is based on sideslip and yaw rather than the desired steer angle, δ. However, it is possible to relate the desired yaw rate, $\dot{\psi}_{target}$, to δ according to

$$\dot{\psi}_{target} = \frac{\dot{x}}{\ell_f + \ell_r + \frac{m\dot{x}^2(\ell_r C_r - \ell_f C_f)}{2C_f C_r(\ell_f + \ell_r)}}\delta \tag{8}$$

where C_f and C_r are the cornering stiffness of the front and rear tires. To ensure vehicle stability during the recovery process, it is desired that the vehicle sideslip remain approximately zero, $\beta_{target} = 0$, so that

$$\dot{s} = \ddot{\psi} - \ddot{\psi}_{target} + \xi\dot{\beta} = -\eta s \tag{9}$$

where $\ddot{\psi}$ can be found from (3). Assuming that the ratio of the front-to-rear brake force distribution, ρ, is constant, $F_{xrl} = \rho F_{xfl}$ and $F_{xrr} = \rho F_{xfr}$. Next, denoting the yaw moment as $M_{\psi b} = \frac{\ell_w}{2}(F_{xfr} - F_{xfl})$ yields the control law

$$\begin{aligned} M_{\psi b} = \frac{I_z}{\rho + \cos(\delta)}\Big[&- \frac{\ell_f}{I_z}(F_{yfl} + F_{yfr})\cos(\delta) \\ &+ \frac{\ell_r}{I_z}(F_{yrl} + F_{yrr}) - \eta s + \ddot{\psi}_{target} - \xi\dot{\beta}\Big]. \end{aligned} \tag{10}$$

This control law is a function of vehicle variables such as sideslip angle, sideslip rate, and front and rear lateral tire forces which cannot be directly measured. Hence, estimation methods are implemented to approximate these values and then they are supplied to the controller.

Now that a control law has been defined for the yaw moment, the braking controller must calculate the corresponding brake pressure at each wheel. Rearranging the expression for the yaw moment reveals the differential longitudinal tire force required to obtain the desired yaw moment, $\Delta F_{xf} = \frac{2M_{\psi b}}{l_w}$. Since the front-to-back distribution of the brake torque has been assumed constant, it is sufficient to examine the dynamics of the front wheels given by

$$J_w\dot{\omega}_{fl} = T_{dfl} - A_w\mu_b R_b P_{bfl} - r_{eff}F_{xfl} \tag{11}$$

$$J_w\dot{\omega}_{fr} = T_{dfr} - A_w\mu_b R_b P_{bfr} - r_{eff}F_{xfr} \tag{12}$$

where the first term on the right side of the equation represents the drive torque, the middle term denotes the braking torque, τ_{brake}, and the final term accounts for the longitudinal tire force torque. The parameters r_{eff}, A_w, μ_b, and R_b denote the effective tire radius, brake area of the wheel, brake friction coefficient, and brake radius, respectively. For minimized wheel sideslip angles it is reasonable to assume that the left and right wheel angular acceleration are equal, $\dot{\omega}_{fl} = \dot{\omega}_{fr}$. Thus, the desired differential longitudinal tire force can be satisfied with the following front left and right brake pressures

$$P_{bfl} = \kappa\frac{\Delta F_{xf} r_{eff}}{A_w\mu_b R_b}, \quad P_{bfr} = (1-\kappa)\frac{\Delta F_{xf} r_{eff}}{A_w\mu_b R_b}. \tag{13}$$

The term $\kappa = \left[\begin{smallmatrix} 1, & M_{\psi b} > 0 \\ 0, & M_{\psi b} \leq 0 \end{smallmatrix}\right]$ activates either the left-side or right-side brakes, depending on the required $M_{\psi b}$.

It was necessary to establish bounds on the steering angle and brake pressures since infinite control gains were unrealistic. The steering bound may be set less than or equal to the maximum allowable steer angle obtainable by the vehicle's steering system. Brake pressure limitations may be set based on system capabilities; however, the differential braking system would likely act in conjunction with an ABS controller, thus brake pressures would be bounded based on wheel slip.

The parameters used in this study have been listed in Table I. The front cornering stiffness, C_f, varied based on the surface friction coefficient, μ_i. The lane-keeping controller parameters, k and x_{la}, were adopted from [7]. The maximum brake pressure, $P_{b,i,max}$, was chosen as the largest possible applied pressure without causing wheel lockup under all road surface conditions. The controller utilized conservative braking forces, which helped to maintain vehicle stability and steerability under low traction conditions. The brake proportioning was set to provide the maximum amount of total braking force possible, and the maximum steer angle, was chosen to approximate standard steering system limitations. Finally, a range of controller gains η and ξ were tested with the ideal value of each used in the study.

TABLE I: Summary of values used for ROR controllers

Parameter	Value	Parameter	Value
m	$1,653kg$	ξ	0.1
I_z	$2,765kg-m^2$	η	5
ℓ_f	$1.4m$	ρ	1
ℓ_r	$1.65m$	r_{eff}	$0.359m$
ℓ_w	$1.55m$	A_w	$1m^2$
δ_{max}	$900deg$	$P_{b,i,max}$	$10MPa$
$C_f(\mu_i = 0.4)$	$20,000N/rad$	μ_b	0.9
$C_f(\mu_i = 0.7)$	$36,500N/rad$	R_b	$0.16m$

B. State Flow Controller

The second proposed controller was an event driven, discrete mode controller that utilized predetermined states to provide the appropriate output. The controller transitioned from state to state using user-defined logic expressions. As discussed previously, the optimal recovery of an ROR situation requires different steering and braking levels applied at

various vehicle operating states (refer to Fig. 1). For this reason, separate but cooperative steering and braking SF controllers were the optimal choice.

Control of the steering angle, δ, was chosen as the primary method for vehicle recovery. The basic SF controller structure was developed using various 'states', $S_\delta = \{Zero, Yaw, Nominal, Sideslip\}$, to determine the output.

Zero State: At each time step, the steering controller begins in the Zero state where no steer angle is commanded. During an ROR event, the controller status is switched on and the controller transitions to either the Yaw or Nominal state depending on the magnitude of the yaw angle, ψ, with relation to the yaw angle threshold, $\psi_{threshold} = 6°$.

Yaw State: Initial correction of the vehicle's trajectory is accomplished in the Yaw state if large yaw angles are experienced as the vehicle leaves the roadway. During this transition, it is critical to minimize the vehicle's lateral position error, e, while limiting sideslip angle, β. The Yaw state is only used while one wheel is off the roadway; once two or more wheels are off, the controller transitions to the Nominal state for steering correction. The commanded steer angle for the Yaw state is a function of the yaw angle, ψ, such that $\delta = K_\psi \cdot \psi$ with a control gain of $K_\psi = 6.5$.

Nominal State: The Nominal state steers the vehicle back onto the center of the roadway lane, while ensuring that the vehicle remains parallel to the road. The requirements for this state are very similar to the tasks performed by the L-K controller. The commanded steer angle for the Nominal state is based on $\delta = K_{Nom} \cdot \delta_{L-K}$ where the control gain $K_{Nom} = 1.2$ and δ_{L-K} is the steer angle commanded by the L-K controller from (6). If, during the vehicle recovery, a large sideslip angle, β, is induced, the controller moves into the Sideslip state.

Sideslip State: In split-μ driving situations, large sideslip angles are often induced due to unequal tire forces on each side of the vehicle. Tire traction is limited at large sideslip angles which can quickly lead to vehicle instability. Increasing the amplitude and response time of the steering command is one method for mitigating large sideslip angles. The commanded steering angle is defined as $\delta = K_\beta \cdot \delta_{L-K}$; however, the control gain, $K_\beta = 1.6$, is chosen to be larger than K_{Nom}, resulting in larger steering inputs. It is necessary to distinguish between the Nominal and Sideslip states because the use of a larger control gain in all situations results in increased vehicle instability and over-correction, causing the vehicle to cross into the opposing lane of traffic. The sideslip threshold was set at $\beta_{threshold} = 2.86°$.

A different braking strategy was used for the SF controller when compared to the SM algorithm described earlier. Braking was performed only when the vehicle's speed was above a set threshold, $V_{threshold} = 55km/h$, and at least one wheel was off of the roadway. This strategy was adopted for three reasons. First, the threat of instability increases at high velocities so reduction of speed is a primary concern, especially before applying steering commands on lower friction surfaces. Second, available tire forces for braking are limited during the stages where the steering commands require most of the tire traction. Third, this strategy helps reduce the overall complexity of the SF controller. Braking was accomplished using separate but identical brake controller designs for each wheel's brake actuator. Using an independent brake system helps increase the vehicle's stability during surface transitions. The SF braking controller consists of three states, $S_{brake} = \{Zero, Full, Small\}$.

Zero State: The controller's default state results in no braking action, $T_{br} = 0Nm$. The brake controller returns to the Zero state if an ROR event is not detected, the vehicle speed is below the speed threshold, $V_{CG} < V_{threshold}$, or all four wheels return to the roadway.

Full State: The Full state is entered when the magnitude of the yaw angle is below $\psi_{threshold}$. Small yaw angles signify little need for cornering ability, thus a large braking torque, $T_{br} = 150Nm$, can be applied to significantly reduce the longitudinal speed.

Small State: In the event that a given wheel begins to lock up, $\omega_i \approx 0$, or if the yaw angle exceeds the threshold, the braking controller changes to the Small state. In this state, a reduced braking torque, $T_{br} = 60Nm$, provides minor speed reduction while allowing for greater cornering ability and reduced possibility of wheel slip.

The wheel steering angle, δ, and individual brake torques, T_{br}, are bounded to remain within the limits of their individual systems. The controller gains, K_ψ, K_{Nom}, and K_β, as well as SF braking forces, were chosen using an iterative calibration process to maximize controller performance.

IV. Driver-Vehicle Reference Model

A numerical based model of typical driver and vehicle behavior in an ROR event was desired to evaluate and compare the performance of the proposed controllers. Therefore, an ROR simulation was created using Matlab and the vehicle dynamics simulation software, CarSim. The CarSim vehicle dynamics have been shown to be reliable and accurate [18], yet further validation was desired to ensure that the simulated vehicle response matched that of a real vehicle's response under typical driver reactions in an ROR event. Experimental data was collected through in-vehicle testing at the Michelin Laurens Proving Grounds (LPG) in Laurens, SC using a four-door sports sedan (BMW 325i).

The vehicle was equipped with sensors and VBOX instrumentation to collect a variety of data including vehicle speed, individual wheel speeds, yaw rate, three-axis accelerations, steering wheel angle, throttle percentage, and brake pressure. The track included dry, slightly worn asphalt with a $2.5cm$ roadway edge drop-off onto a grassy shoulder. An expert driver was instructed to steer off the test track into a two-wheels-off position and recover the vehicle using a typical immediate overcorrection and elongated counter-steer technique exhibited by most inexperienced drivers. No braking was used in the recovery process as drivers typically focus entirely on steering the vehicle back onto the roadway [19]. The recorded data, along with external video footage, served as the reference by which to validate the simulation model.

A virtual road environment was created in CarSim to closely replicate the LPG track. The simulation included a lip height between the road surface and shoulder of $h_{diff} = 0.025m$, surface frictions of $\mu_{road} = 0.7$ and $\mu_{shoulder} = 0.4$, and an initial vehicle velocity $V_{CG} = 75km/h$. For comparison, the simulated vehicle was brought into a two-wheels-off position and the driver steering inputs recorded from the LPG test were fed to the simulation to observe the vehicle response. The simulated data was then evaluated against the test data. The maximum lateral displacement, $y_{CG,max}$, of the test track vehicle was $9m$ while the simulation shows a max vehicle displacement of $y_{CG,max} = 8.5m$, less than a 10% difference.

To supplement the lateral displacement analysis, a comparison of the vehicle yaw rate and lateral CG acceleration was performed. Fig. 2 shows that the transient behavior of the two vehicles exhibit similar trends; however, the peak magnitudes of the test track data tend to exceed the simulation data at a few specific intervals. During the vehicles' initial departure from the roadway, the LPG data shows a large peak in the yaw rate and a lateral acceleration 0.5g's above the simulation data. However, the data sets correspond well as the vehicles transition onto the shoulder, while on the shoulder, and as they transition back to the roadway. Once the vehicles return to the road, the lateral acceleration of the LPG vehicle is again 0.5g's larger in magnitude than the simulation. The contrasts in data can primarily be attributed to modeling limitations specifically with the vehicle and tires. The closest vehicle to the BMW 3 series which could be readily modeled in CarSim was a Mercedes C-Class. The BMW also had performance tires whereas the simulated Mercedes did not. Independent source testing shows that the peak performance of a BMW 3 series with nonperformance tires is around 0.75g's [20] which is much closer to the simulation values. Thus, the differences in these two vehicles and their tires likely accounts for the reduced peak performance capabilities of the simulated vehicle. The simulated ROR vehicle model has therefore been established as a reasonable method for testing the performance of the developed ROR controllers.

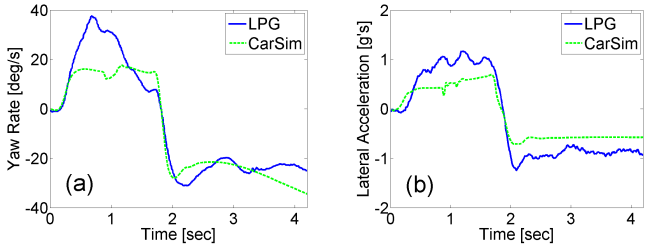

Fig. 2: Vehicle (a) yaw rate and (b) lateral acceleration from field testing at Laurens Proving Grounds compared to the CarSim simulation

V. Numerical Results

To evaluate the control designs, the simulated vehicle was programmed to deviate from the roadway and the controllers attempted to recover the vehicle. The results were compared to a driver model (DM) representing the response of a typical inexperienced driver. The DM was created by supplying the driver steering inputs obtained from the LPG data into the simulation. Ideally, the recovery process would use as little steering angle as possible to promptly return the vehicle back to the road, while maximizing stability. Therefore, the performance of each ROR recovery was judged based on steering wheel angle, sideslip, lateral vehicle motion, Y_{CG}, and time/distance for vehicle recovery as shown in Fig. 3. The values t_{rd} and x_{rd} represent the time and distance required to bring all four wheels back onto the roadway, while t_{rec} and x_{rec} are the time and distance required to fully recover the vehicle to its original desired path. The right and left lateral errors, $e_{r,max} = |MIN(Y_{CG} - Y_{LC})|$ and $e_{l,max} = |MAX(Y_{CG} - Y_{LC})|$, are examined since large values signify an increased danger to the vehicle and its occupants. An evaluation of the total lateral position error is accomplished using a root-mean-square (RMS) methodology given as $e_{RMS} = \sqrt{\frac{\sum_{i=1}^{n} e_{la,i}^2}{n}}$ where n is the total number of data points and $e_{la,i}$ is the instantaneous lane offset error.

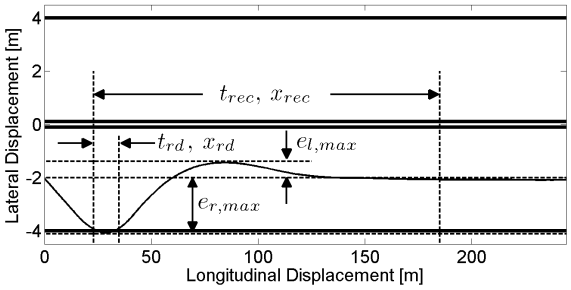

Fig. 3: Visual representation of controller performance metrics

Implementation of the two controllers was simulated under identical conditions, $V_{CG} = 85km/h$, $\Delta\mu = 0.3$ ($\mu_{shoulder} = 0.4$ and $\mu_{road} = 0.7$), $h_{diff} = 0.025m$, and $\delta_{init} = 10°$. The displacement results of the simulation are shown in Fig. 4. It is first noted that the DM and both controllers were successful at returning the vehicle to the roadway; however, only the controllers were successful at maintaining vehicle stability and maneuvering the vehicle back into the proper lane. After returning to the roadway, the DM applied large elongated steering inputs in an attempt to keep the vehicle in the proper lane. The large steering inputs induced high sideslip angles, $\beta > 6°$, causing the tires to lose frictional contact, thus resulting in the vehicle spinning out of control. The DM's loss of stability caused it to have the largest $e_{l,max} = 3.71m$, placing the vehicle in the middle of the opposing lane of traffic. The SF controller performed the best in terms of minimizing the lateral error with an $e_{RMS} = 1.02$ versus the SM controller with an $e_{RMS} = 1.19$. The SF controller was also the quickest to return the vehicle back to the roadway with $t_{rd} = 1.52s$ and $x_{rd} = 34.59m$ compared to the DM at $1.66s$ and $37.97m$

and the SM controller at $1.98s$ and $45.74m$. Fig. 4 also shows that the SF controller performs the entire recovery faster with $t_{rec} = 5.66s$ and $x_{rec} = 116.97m$ whereas the SM controller takes $9.78s$ and $210.51m$.

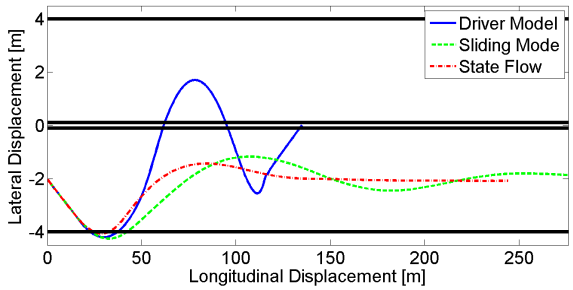

Fig. 4: Vehicle displacement with road centerline at $Y = 0m$, shoulders at $Y = \pm 4m$, and lane center at $Y = -2m$

Fig. 5 displays the steering inputs commanded in each simulation. The DM used the largest peak steering input, nearly six to ten times more than the SF and SM controllers. In all three simulations, maximum steering angles occur as the controller or driver initially attempts to return the vehicle back onto the roadway. Once the initial recovery is made, both the SM and SF controllers use smaller steering inputs to settle the vehicle into the proper lane position. The controllers' smaller steering inputs resulted in smaller sideslip and yaw angles. The SF controller used slightly more aggressive steering resulting in $\beta_{max} = -2.79°$ and $\psi_{max} = 13.45°$ versus the SM controller with $\beta_{max} = -0.45°$ and $\psi_{max} = 7.23°$.

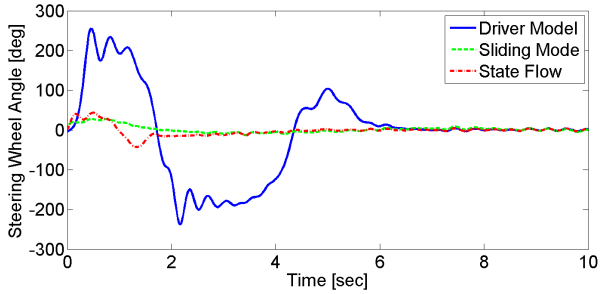

Fig. 5: Steering wheel angle, θ, used during ROR recovery

In summary, both ROR controllers successfully recovered the vehicle and outperformed the DM. The SF controller recovered faster than the SM controller, but at the cost of larger steering inputs and thus larger yaw and sideslip angles.

VI. Conclusion

One of the most dangerous types of vehicle incidents is a run-off-the-road situation. Too often it is the driver's delayed response and poor performance during recovery which cause unfavorable or even fatal outcomes. In this study, two separate controllers (sliding mode and state flow) have been developed for the autonomous recovery of a vehicle in an ROR situation using combined steering and differential braking inputs. The two controllers outperformed a driver model by safely returning the vehicle into the correct lane and angular orientation without loss of stability or excessive lane error. While commercial implementation of such autonomous controllers may be premature, a tremendous need exists for both on-board control systems and driver training to improve the survivability of this dangerous scenario.

References

[1] National Highway Traffic Safety Administration, "Traffic safety facts 2008: A compilation of motor vehicle crash data from the Fatality Analysis Reporting System and the General Estimates System," U.S. DOT, Washington, DC, Rep. DOT HS 811 170, 2009.

[2] C. Liu and T. Ye, "Run-off-road crashes: An on-scene perspective," NHTSA, Washington, DC, Rep. DOT HS 811 500, July, 2011.

[3] S. Levett, "Retro-fitting road safety to existing rural roads," in *Local Road Safety and Traffic Engineering Conf.*, Gold Coast, Australia, 2007, pp. 1-17.

[4] D. Morena, "The nature and severity of drift-off road crashes on Michigan freeways, and the effectiveness of various shoulder rumble strip designs," in *Proc. 2003 Transportation Research Board*, TRB 2003-001252, Washington, DC.

[5] D. Marzougui, P. Mohan, C. Kan, and K. Opiela, "Performance evaluation of low-tension three-strand cable median barriers," *J. Transport. Research Board*, vol. 2025, pp. 34-44, 2007.

[6] P. Deram, "Vehicle based detection of inattentive driving for integration in an adaptive lane departure warning system - Distraction detection," M.S. thesis, Dept. Sig., Sens. & Syst., Royal Inst. of Tech., Stockholm, Sweden, 2004.

[7] E. Rossetter, J. Switkes, and J. Gerdes, "A gentle nudge towards safety: Experimental validation of the potential field driver assistance system," in *Proc. American Control Conf.*, Denver, CO, June, 2003.

[8] E. Rossetter, and J. Gerdes, "Lyapunov based performance guarantees for the potential field lane-keeping assistance system," *J. of Dynam. Syst., Meas., and Contr.*, vol. 128, no. 3, pp. 510-522, Sept. 2006.

[9] J. Black, J. Wagner, K. Alexander, and P. Pidgeon, "Vehicle road runoff - Active steering control for shoulder induced accidents," in *Proc. American Control Conf.*, Seattle, WA, 2008, pp. 3237-3244.

[10] R. Rajamani, "Electronic stability control," in *Vehicle dynamics and control*, New York: Springer, 2006, pp. 221-256.

[11] P. Yih, and J. Gerdes, "Modification of vehicle handling characteristics via steer-by-wire," *IEEE Trans. Contr. Syst. Tech.*, vol. 13, no. 6., pp. 965-976, Nov. 2005.

[12] S. Underwood, A. Khalil, I. Husain, H. Klode, B. Lequesne, S. Gopalakrishnan, and A. Omekanda, "Switched reluctance motor based electromechanical brake-by-wire system," *Int. J. Vehicle Auton. Syst.*, vol. 2, no. 3-4, pp. 278-296, 2004.

[13] W. Xiang, P. Richardson, C. Zhao, and S. Mohammad, "Automobile brake-by-wire control system design and analysis," *IEEE Trans. Vehicular Tech.*, vol. 57, no. 1, pp. 138-145, Jan. 2008.

[14] S. Anwar, "A parametric model of an Eddy Current electric machine for automotive braking applications," *IEEE Trans. Contr. Syst. Tech.*, vol. 12, no. 3, pp. 422-427, May 2004.

[15] J. Slotine and W. Li, "Sliding control," in *Applied nonlinear control*, New Jersey: Prentice Hall, 1991, pp. 276-310.

[16] K. Uematsu and J. Gerdes, "A comparison of several sliding surfaces for stability control," in *Proc. Int. Symp. Advanced Vehicle Control*, 2002.

[17] K. Yi, T. Chung, J. Kim, and S. Yi, "An investigation into differential braking strategies for vehicle stability control," *Proc. Inst. Mech. Eng., Part D: J. Automobile Eng.*, vol. 217, pp. 1081-1093, 2003.

[18] T. Kinjawadekar, N. Dixit, G. Heydinger, D. Guenther, and M. Salaani, "Vehicle dynamics modeling and validation of the 2003 Ford Expedition with ESC using CarSim," *SAE technical paper* 2009-01-0452, 2009.

[19] AAA Foundation for Traffic Safety. (2006). Over the edge and back. [Online]. Available: http://www.aaafoundation.org/pdf/PEDO_brochure.pdf

[20] M. Allen. (2010, July 16). Tire comparison test: What rubber should you choose?. *Popular Mechanics* [Online]. Available: http://www.popularmechanics.com/cars/howto/products/best-tire-brand-comparison-test-2